Dependence of Interfacial Dzyaloshinskii-Moriya Interaction on Layer Thicknesses in Ta/Co-Fe-B/TaO_x Heterostructures from Brillouin Light Scattering

Avinash Kumar Chaurasiya, Samiran Choudhury, Jaivardhan Sinha, and Anjan Barman*

Department of Condensed Matter Physics and Material Sciences, S. N. Bose National Centre for Basic Sciences, Block JD, Sec. III, Salt Lake, Kolkata 700106, India

(Received 27 July 2017; revised manuscript received 30 October 2017; published 10 January 2018)

The interfacial Dzyaloshinskii-Moriya interaction (IDMI) has recently drawn extensive research interest due to its fundamental role in stabilizing chiral spin textures in ultrathin ferromagnets, which are suitable candidates for future magnetic-memory devices. Here, we explore the ferromagnetic and heavy-metal layer-thickness dependence of IDMI in technologically important Ta/$Co_{20}Fe_{60}B_{20}$/TaO_x heterostructures by measuring nonreciprocity in spin-wave frequency using the Brillouin light-scattering technique. The observed value of the IDMI constant agrees with that obtained from a separate measurement of in-plane angular dependence of frequency nonreciprocity, which is also in good agreement with the theory predicted by Cortes-Ortuno and Landeros. Linear scaling behavior of IDMI with the inverse of Co-Fe-B thicknesses suggests that IDMI originates primarily from the interface in these heterostructures, whereas we observe a weak dependence of Ta thickness on the strength of IDMI. Importantly, the observed value of the IDMI constant is reasonably large by a factor of 3 compared to annealed Ta/Co-Fe-B/MgO heterostructures. We propose that the observation of large IDMI is likely due to the absence of boron diffusion towards the Ta/Co-Fe-B interface as the heterostructures are as deposited. Our detailed investigation opens up a route to designing thin-film heterostructures with the tailored IDMI constant for controlling Skyrmion-based magnetic-memory devices.

DOI: 10.1103/PhysRevApplied.9.014008

I. INTRODUCTION

Because of the ever-increasing demand of data storage and processing, much attention is being paid by the scientific community to searching for new materials and physics for future storage, memory, logic, and communication devices. In such a context, broken inversion symmetry systems have emerged as potential candidates which show striking features like Dzyaloshinskii-Moriya interaction (DMI), which originates due to the breaking of structural inversion symmetry at the interface of heavy metal (HM) possessing strong spin-orbit coupling and ferromagnet (FM) [1–4]. Basically, DMI is an antisymmetric component of an interatomic magnetic exchange which favors chiral structure, whereas the symmetric component is commonly known as the Heisenberg exchange interaction that stabilizes spatially uniform magnetization. More recently for application in magnetic-memory devices, new concepts have been proposed based on the spin Hall effect [5,6], perpendicular magnetic anisotropy [7,8], the Rashba effect [9], and interfacial DMI (IDMI) [10]. A firm understanding and tunability of IDMI may facilitate the design of the next-generation magnetic memory and logic devices based on the chiral magnetic domain walls and Skyrmions [10–13]. Achieving the large velocity of the domain wall by means of current control is envisioned to be useful in high-density racetrack memory [14]. Although, the phenomenon of DMI was predicted two decades ago, its experimental realization has only been possible in ultrathin-film heterostructures during the last few years. It has been reported that IDMI leads to spin spiral in Mn monolayers on W(110) [15], nanoscale Skyrmion lattices in Fe monolayers on Ir (111) [16], and isolated Skyrmion on Pd/Fe bilayers on Ir (111) [17]. Moreover, fast current-induced magnetic domain-wall motion has recently been explored via the combination of chiral domain-wall structure and spin-orbit torque where the chirality and speed of the domain-wall motion depend on the sign, the magnitude of the IDMI, and the spin-orbit torque [11]. It is expected that the interfacial DMI at HM-FM interface would show a large sensitivity to the choice of both the HM and FM layers. An interesting theoretical study has recently proposed that IDMI affects predominantly the interfacial spins in the FM layer and extends weakly in the FM and HM layers [18]. It is understood that intermixing at the HM-FM interface is detrimental for achieving large IDMI. Furthermore, the strength and the sign of IDMI in multilayered structures is greatly affected by the material composition, stack order, interface quality, etc. [19]. The tunability in these parameters may provide an efficient way to control the IDMI.

Previous measurements of the quantification of DMI are reported using spin-polarized scanning tunneling microscopy

*abarman@bose.res.in

[15], highly resolved spin-polarized electron-energy-loss spectroscopy [20], scanning-nitrogen-vacancy magnetometry [21], synchrotron-based x-ray scattering, current-induced magnetic domain-wall dynamics [22], and asymmetric magnetic nucleation measurements [23]. Moreover, numerical and analytical micromagnetics have also been implemented to study DMI [24,25]. More recently, the direct observation of IDMI using the Brillouin light-scattering (BLS) technique has been demonstrated [26–30]. An important thin-film heterostructure Ta/Co-Fe-B/TaO_x has been studied by Yu *et al.* [31] in the context of switching of perpendicular magnetization by spin-orbit torque in the absence of magnetic field. Furthermore, it has been shown that the chiral magnetic bubbles can be nucleated in Ta/Co-Fe-B/TaO_x heterostructures suggesting the presence of the IDMI [32]. Recent experimental investigations show the ferromagnetic layer-thickness dependence of the strength of IDMI demonstrating $1/t$ behavior. (where t is the ferromagnetic layer thickness) [29]. In the Pt/(Co-Fe-B)-based system, the IDMI constant has been reported to show an interesting nonlinear dependence on Pt thickness. Specifically, the IDMI constant has been found to increase with Pt thickness below its spin-diffusion length, whereas above the spin-diffusion length it saturates [33]. In order to gain a deep understanding regarding IDMI in Ta/Co-Fe-B/TaO_x thin-film heterostructures, a systematic study is needed. However, a systematic study of the influence of FM and HM layer thicknesses on the strength of IDMI in these heterostructures is still missing in the literature.

In this article, we present a systematic study of FM and HM layer-thickness dependence of IDMI in technologically important Ta/$Co_{20}Fe_{60}B_{20}$/TaO_x heterostructures from asymmetric spin-wave dispersion probed by the BLS technique. We observe a reasonably large IDMI value originating primarily from the interface in these heterostructures. Further confirmation of the IDMI constant is evidenced by performing the in-plane angular dependence of the frequency nonreciprocity of Ta/$Co_{20}Fe_{60}B_{20}$/TaO_x thin-film heterostructures, which is in good agreement with the analytical theory formulated by the Cortes-Ortuno and Landeros [34] for the dispersion relations of the spin waves in ferromagnetic thin films with DMI.

II. EXPERIMENTAL DETAILS

A series of samples consisting of substrate/Ta(d)/$Co_{20}Fe_{60}B_{20}$(1 nm)/TaO_x(0.5 nm), with $d = 0$, 0.5, 0.8, 1, 2, 3, 4, 5, 6 nm and substrate/Ta(2 nm)/$Co_{20}Fe_{60}B_{20}$(t)/TaO_x(0.5 nm), with $t = 0.85$, 1, 1.5, 2, 3 nm are deposited by dc-rf magnetron sputtering on a Si (100) wafer coated with 100-nm-thick SiO_2 at room temperature. The base pressure of the chamber is better than 2×10^{-7} Torr and the uniformity in the thickness of the layer is ensured by rotating the substrate at 10 rpm during deposition. Ta is grown using a rf power of 40 W, whereas for Co-Fe-B, a dc power of 38 W is used. All of these films are grown in an Ar gas atmosphere of 1-mTorr pressure. The vibrating sample magnetometer (VSM) measurement is performed to estimate the values of saturation magnetization (M_s). Importantly, all these films are in-plane magnetized as revealed by VSM measurement.

In order to investigate the asymmetric spin-wave dispersion caused by IDMI, BLS measurements are performed in Damon-Eshbach geometry using a Sandercock-type six-pass tandem Fabry-Pérot interferometer. Conventional 180° backscattered geometry is used along with the provision of wave-vector selectivity to investigate the spin-wave dispersion relation. In the light-scattering process, total momentum is conserved in the plane of the thin film. As a result, the Stokes (anti-Stokes) peaks in BLS spectra correspond to the creation (annihilation) of magnons with momentum $k = [(4\pi)/\lambda] \sin\theta$, where λ is the wavelength of the incident laser beam (532 nm in our case), and θ refers to the angle of incidence of laser. To get well-defined BLS spectra for the larger incidence angles, the spectra are obtained after counting photons for several hours. A free spectral range (FSR) of 50 GHz and a 2^9 multichannel analyzer are used during the BLS measurement. The frequency resolution is determined by estimating FSR/2^9 ($\approx$0.1 GHz) for the Stokes and anti-Stokes peaks of the BLS spectra. In the second part of the BLS experiment, the sample and the magnet are mounted on a two-axis translation stage, thereby allowing the variation in the in-plane angle between the applied magnetic field H and the spin-wave wave vector k. The translation stage is attached to a vertically mounted rotation stage making their axes orthogonal, allowing θ to be set at 45° (in our case). Using this arrangement, we measure the asymmetry in the spin-wave frequency as a function of the angle (ϕ) between the applied bias field and the wave vector k.

III. RESULTS AND DISCUSSIONS

Figure 1(a) represents the grazing incidence x-ray diffraction (GIXRD) patterns for the sample: substrate/Ta(6 nm)/Co-Fe-B(1 nm)/TaO_x(0.5 nm). From the analysis of the XRD data, it is revealed that the peak (002) at 35.4° corresponds to the β-Ta phase. Furthermore, TaO_x peaks with lower intensity and Si substrate peaks are also identified and marked in the figure. These findings are consistent with the existing literature reports [35,36]. Figure 1(b) shows the atomic force microscope (AFM) images for the sample Ta(d)/Co-Fe-B(1 nm)/TaO_x(0.5 nm) with $d = 1$ and 6 nm. The average topographical roughness for all films is in the range of 0.20 to 0.25 nm. To extract the magnetic parameters, we perform the magnetic field dependence of the spin-wave frequency. Figure 1(c) represents the typical BLS spectra measured at normal incidence ($k \approx 0$, corresponding to the uniform precessional mode) at various in-plane applied magnetic field (H) for Ta(2 nm)/Co-Fe-B(2 nm)/TaO_x(0.5 nm). The value of H is mentioned on each spectrum. The BLS

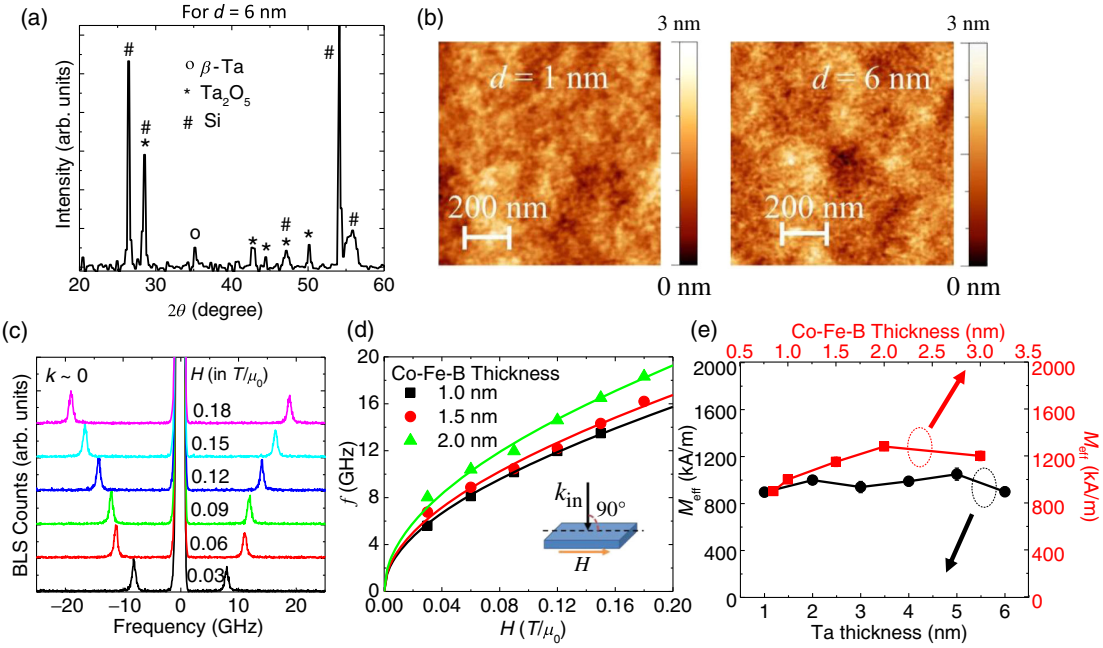

FIG. 1. (a) Grazing incidence x-ray diffraction (GIXRD) pattern for the sample Ta(6 nm)/Co-Fe-B(1 nm)/TaO_x(0.5 nm) grown on Si (100) substrate. (b) Atomic-force-microscope image of Ta(d)/Co-Fe-B(1 nm)/TaO_x(0.5 nm) (where $d = 1$ and 6 nm). (c) Representative BLS spectra measured for Ta(2 nm)/Co-Fe-B(2 nm)/TaO_x(0.5 nm) for various in-plane applied field at $k \sim 0$. Digits mentioned above each spectrum refer to the magnetic field in T/μ_0. (d) Plot of frequency (f) vs magnetic field (H) for the film stack Ta(2 nm)/Co-Fe-B(t)/TaO_x(0.5 nm) with $t = 1$, 1.5, and 2 nm. Symbols represent the experimentally measured data points, whereas the solid curve is the fit using Eq. (1). Inset: Schematic of the measurement geometry. (e) Plot of M_{eff} vs Ta thickness for film stack Ta(d)/Co-Fe-B(1 nm)/TaO_x(0.5 nm) (left and bottom axes) and Co-Fe-B thickness Ta(2 nm)/Co-Fe-B(t)/TaO_x(0.5 nm) (right and top axes).

spectra are well fitted with the Lorentzian function to get the frequency value (f) which increases with increasing H. In Fig. 1(d), f as a function of H is shown for the samples with $t = 1$, 1.5, and 2 nm. The standard Kittel formula [cf. Eq. (1)] is used to fit these experimental data.

$$f = \frac{\mu_0 \gamma}{2\pi}[H(H + M_{\text{eff}})]^{1/2}. \tag{1}$$

Here, $\gamma = g\mu_B/h$, g is the Landé g factor, and M_{eff} is the effective magnetization. We use $\mu_0 = 4\pi \times 10^{-7}$ N/m^2 as the vacuum permeability and determine g and M_{eff} as fitting parameters. The best fit to the data yields $g = 2.00 \pm 0.05$ for all the samples. The plot of M_{eff} vs Ta underlayer thickness [Ta(d)/Co-Fe-B(1 nm)/TaO_x(0.5 nm), bottom and left axes] and Co-Fe-B layer thickness [Ta(2 nm)/Co-Fe-B(t)/TaO_x(0.5 nm), top and right axes] is shown in Fig. 1(e). Extracted values of M_{eff} are close to the values of saturation magnetization (M_s) measured using VSM for almost all film stacks, thus indicating negligibly small interface anisotropy. It is worth mentioning here that since all of these films are unannealed, the presence of interface anisotropy is ruled out in these stacks.

To investigate the IDMI in these thin-film heterostructures, we measure the spin-wave dispersion (f vs k) relation at the applied in-plane field of 0.1 T/μ_0. Here, k is varied by changing the angle of incidence of the laser beam. Since the thickness of the Co-Fe-B is much smaller than the optical skin depth of the metal, the spin waves propagating in the opposite directions are simultaneously detected as Stokes and anti-Stokes peaks in the BLS spectra. In order to model our experimental data, we use the equation for the difference in the frequencies of counterpropagating spin waves given below [26,29]

$$\Delta f(k) = [\omega(-k) - \omega(k)]/2\pi = \frac{2\gamma}{\pi M_S} Dk, \tag{2}$$

which is linear in D and k. Here, D is the IDMI constant. Therefore, Eq. (2) provides an elegant way to quantify the strength of IDMI by experimentally measured quantities Δf, M_s, and k. Typical BLS spectra recorded at a higher wave vector ($k = 2.04 \times 10^7$ rad/m) for different thicknesses of Co-Fe-B are presented in Fig. 2(a). Note that the BLS measurement is performed in Damon-Eshbach geometry as shown schematically. In all cases, the in-plane applied field is 0.1 T/μ_0. By looking at these BLS spectra, it is evident that the frequency difference between Stokes and anti-Stokes peaks (Δf), which is the measure of the strength of IDMI, increases with decreasing Co-Fe-B thickness. In the case of $t = 0.85$ nm, $\Delta f \approx 0.50$ GHz which is reasonably large for the Ta/Co-Fe-B/TaO_x system.

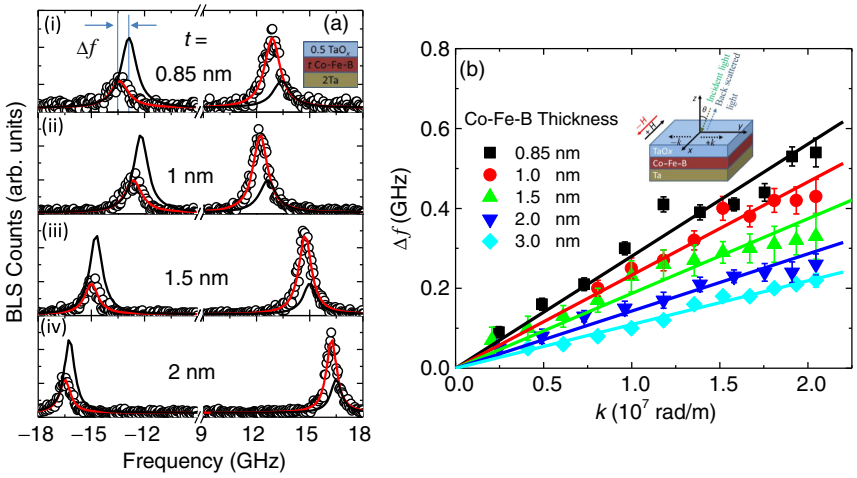

FIG. 2. (a) Representative BLS spectra measured at wave vector $k = 2.04 \times 10^7$ rad/m for the Ta(2 nm)/Co-Fe-B(t)/TaO_x(0.5 nm) sample for two counterpropagating directions. The spectrum corresponding to the particular thickness of Co-Fe-B is indicated by mentioning the thickness value in each panel. The solid curve is the fit using the Lorentzian function. (b) Plot of Δf vs k for Ta(2 nm)/Co-Fe-B(t)/TaO_x(0.5 nm) samples with various values of t. Symbols represent the experimental data points and solid lines are the fit using Eq. (2). Inset: Schematic of the film stack along with BLS geometry.

To get a quantitative estimation of the IDMI, the variation of Δf as a function of k is displayed in Fig. 2(b) for all Co-Fe-B thicknesses studied here. Considering $g = 2$ and taking $M_s = 900$ kA/m obtained from VSM measurement, D is obtained as 0.22 ± 0.03 mJ/m^2 from the slope of the linear correlation using Eq. (2) for the sample with $t = 0.85$ nm. Similar fitting procedures are applied for other thicknesses of Co-Fe-B, and D values are estimated from the slope of the linear fit. We observe that the value of D in these systems is modest in comparison to the Pt/FM system [26]. Nevertheless, the pronounced DMI in our system (Ta/Co-Fe-B) is almost three times higher than earlier reported values [37]. Earlier experimental studies of structural characterization in as-deposited and annealed Ta/Co-Fe-B/MgO have demonstrated that the boron predominantly resides in Co-Fe-B for as-deposited stacks, however, it diffuses out to adjacent layers once the stacks are annealed [37,38]. It has been shown that diffusion of B atoms from Co-Fe-B during the annealing process leads to the decrement in the strength of DMI [37,39], primarily due to the segregation of B atoms at the Ta/Co-Fe-B interface. As the film stacks investigated in the present study are as deposited, hence, we propose that such possibility of B diffusion is likely avoided. A further detailed microstructural study to investigate the presence of boron in as-deposited Ta/Co-Fe-B/TaO_x is needed in the future to verify such a proposition. In general, to achieve large perpendicular magnetic anisotropy and tunnel magnetoresistance Ta/Co-Fe-B/TaO_x stacks are annealed. Apart from boron diffusion, annealing also causes intermixing, which may reduce the IDMI. To cross-check the wave-vector (k) dependent Δf measurements, we also perform asymmetry in the spin-wave frequency as a function of the angle (ϕ) between the bias field and the wave vector k. The relationship between Δf and ϕ is given by Eq. (3) [40]

$$\Delta f(k) = \frac{2\gamma D k}{\pi M_S} \sin\phi. \tag{3}$$

BLS spectra are taken for values of ϕ in the range $-180° \le \phi \le 180°$ at an interval of 10° and at fixed wave vector $k = 1.67 \times 10^7$ rad/m. In Fig. 3(a), typical BLS spectra at various ϕ values are presented for the sample with $t = 1$ nm. It can be noted that Stokes and anti-Stokes peaks clearly appear in the BLS spectrum due to the

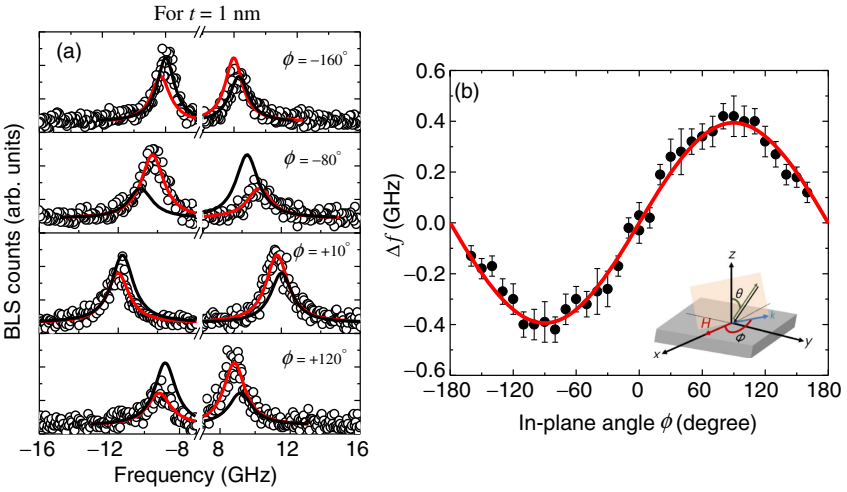

FIG. 3. (a) BLS spectra of Ta(2 nm)/Co-Fe-B(1 nm)/TaO_x(0.5 nm) sample measured under $H = 0.1$ T/μ_0, $k = 1.67 \times 10^7$ rad/m for various in-plane angles ϕ. (b) The variation of frequency difference (Δf) between Stokes and anti-Stokes peak of Ta(2 nm)/Co-Fe-B(1 nm)/TaO_x(0.5 nm) sample with in-plane angle ϕ. Symbols represent the experimental data points and the solid curve is the fit using Eq. (3). Inset: Schematic of the 180° backscattering geometry.

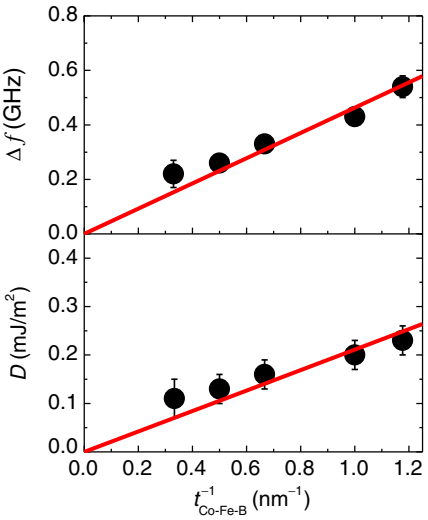

FIG. 4. Variation of Δf (top panel) and D (bottom panel) with the inverse of Co-Fe-B thickness. The error bar in Δf is shown by considering the error from the fitting of spectra as well as the instrumental resolution to determine the peak frequency and for D, errors in M_s as well as Δf have been taken into account. The red solid lines in both the cases are the linear fits.

thinness of the ferromagnetic film. According to Eq. (3), the frequency difference between Stokes and anti-Stokes (Δf) peaks is maximal in the vicinity of $\phi = -90°$ and 90°, whereas it is almost negligible in the vicinity of −180°, 0°, and 180°.

Figure 3(b) shows the variation of Δf as a function of in-plane angle ϕ. To fit the experimental data, we use Eq. (3) with the same fitting parameters (like g and M_s) which is used to fit the experimental data of k-dependent BLS measurements. From the sinusoidal fitting, we extract the value of D as 0.19 ± 0.03 mJ/m^2 which matches reasonably well with the previously obtained value from k-dependent BLS measurements. It is worth mentioning here that the error in D is estimated by considering the experimental uncertainties of Δf, M_s, g, and k. The implementation of this method provides additional confirmation of the reasonably high value of D in these samples.

We next investigate the dependence of the strength of interfacial DMI on FM layer thickness t. Figure 4 shows the variation of Δf measured at $k = 2.04 \times 10^7$ rad/m (top panel) and the deduced IDMI energy density D (bottom panel) with the inverse of Co-Fe-B thickness. It is clear from these plots that both Δf and D increase almost linearly with the decrease in the Co-Fe-B thickness. The best linear fit to the inverse of Co-Fe-B thickness dependence of Δf and D elucidate that both Δf and D approach zero as t tends to infinity, confirming the interfacial origin of DMI in our samples. Importantly, this linear scaling behavior does not deviate even for the subnanometer thickness of Co-Fe-B, which makes it a potentially suitable candidate for spintronic devices utilizing interfacial effects.

To understand the effects of underlayer thickness on the strength of IDMI, we perform the Ta underlayer thickness dependence of IDMI in samples described by substrate/Ta(d)/$Co_{20}Fe_{60}B_{20}$(1 nm)/TaO_x(0.5 nm), with $d = 0$, 0.5, 0.8, 1, 2, 3, 4, 5, 6 nm. To date, not much attention has been paid to exploring the influence of underlayer thickness in the context of IDMI. Recently, Tacchi *et al.* studied the role of Pt thickness on the strength of IDMI in Pt/Co-Fe-B, revealing that D first increases and then saturates with Pt thickness [33]. Figure 5(a) shows the

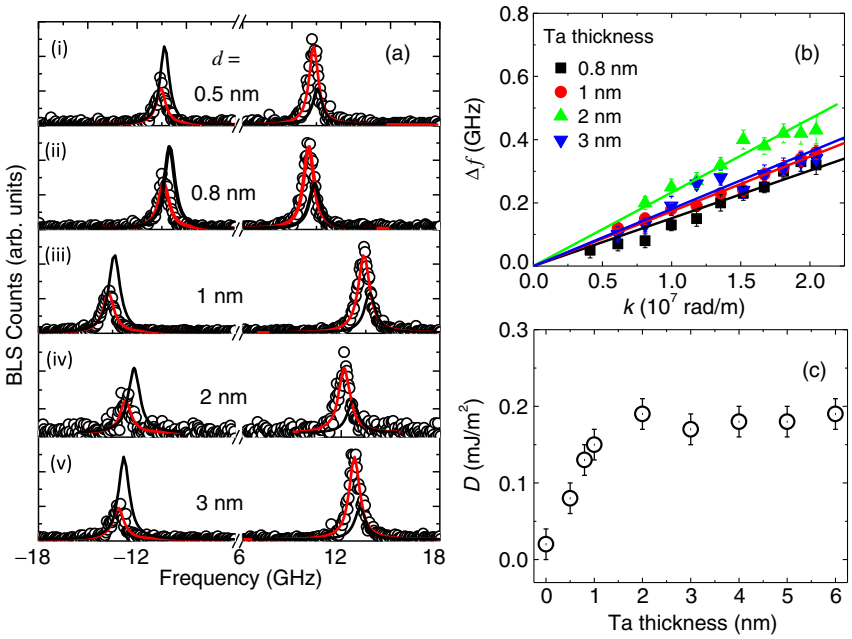

FIG. 5. (a) Representative BLS spectra (i)–(v) measured at wave vector $k = 2.04 \times 10^7$ rad/m for the Ta(d)/Co-Fe-B(1 nm)/TaO_x(0.5 nm) sample for two counterpropagating directions. The spectrum corresponding to the specific thickness of Ta is indicated by mentioning the thickness value in each panel. The solid curve is the fit using the Lorentzian function. (b) Variation of Δf with k for Ta(d)/Co-Fe-B(1 nm)/TaO_x(0.5 nm) samples with various d values. Symbols represent the experimental data points and solid lines are the fit using Eq. (2). (c) Variation of D with the Ta thickness.

typical BLS spectra recorded for various d values at $k = 2.04 \times 10^7$ rad/m. It can be seen that Δf increases slightly as d increases from 0 to 2 nm and then saturates for $d \geq 2$ nm. To obtain the quantitative estimation of D, variation of Δf as a function of k has been presented in Fig. 5(b) for several d values, and the extraction of the D parameter is performed from the linear fit [using Eq. (2)]. In Fig. 5(c) the variation of D with Ta thickness is shown, whose trend resembles well with the recent findings by Tacchi *et al.* [33] in their study of Pt/Co-Fe-B films.

IV. CONCLUSION

In summary, we have systematically studied the FM layer and HM underlayer-thickness dependence of IDMI in technologically important Ta/Co-Fe-B/TaO_x heterostructure using BLS spectroscopy. By measuring the spin-wave frequency nonreciprocity, we observe significantly large IDMI in these stacks likely due to the absence of B diffusion at the Ta/Co-Fe-B interface as these films are unannealed. Furthermore, the presence of large IDMI is also cross verified by the sinusoidal angular dependence of spin-wave nonreciprocity Δf. In the case of FM thickness variation, we observe that D varies linearly with the inverse of Co-Fe-B thickness, demonstrating its purely interfacial origin, whereas in the case of Ta thickness dependence, D shows a sharp variation in the subnanometer thickness range and attains a nearly constant value above a Ta thickness of 1 nm. Our detailed FM and HM thickness-dependent studies will enrich the understanding regarding the tunability of IDMI in these heterostructures for controlling chiral spin structure and magnetic domain-wall-based magnetic storage and memory devices.

ACKNOWLEDGMENTS

We gratefully acknowledge the financial assistance from the Department of Science and Technology (DST), Government of India, under Grant No. SR/NM/NS-09/2011 and the S. N. Bose National Centre for Basic Sciences under Project No. SNB/AB/12-13/96. A. K. C. acknowledges DST, Government of India for support from the INSPIRE Fellowship (No. IF150922) and J. S. acknowledges the DST, Government of India, for support from the Ramanujan Fellowship (No. SB/S2/RJN-093/2014). S. C. acknowledges the S. N. Bose National Centre for Basic Sciences for Senior Research Fellowship.

[1] I. E. Dzyaloshinskii, Thermodynamic theory of weak ferromagnetism in antiferromagnetic substances, Sov. Phys. JETP **5**, 1259 (1957).
[2] T. Moriya, Anisotropic superexchange interaction and weak ferromagnetism, Phys. Rev. **120**, 91 (1960).
[3] A. Fert, V. Cros, and J. Sampaio, Skyrmions on the track, Nat. Nanotechnol. **8**, 152 (2013).
[4] S. Mühlbauer, B. Binz, F. Jonietz, C. Pfleiderer, A. Rosch, A. Neubauer, R. Georgii, and P. Böni, Skyrmion lattice in a chiral magnet, Science **323**, 915 (2009).
[5] L. Liu, C.-F. Pai, Y. Li, H. W. Tseng, D. C. Ralph, and R. A. Buhrman, Spin-torque switching with the giant spin Hall effect of tantalum, Science **336**, 555 (2012).
[6] J. Kim, J. Sinha, M. Hayashi, M. Yamanouchi, S. Fukami, T. Suzuki, S. Mitani, and H. Ohno, Layer thickness dependence of the current-induced effective field vector in Ta|CoFeB|MgO, Nat. Mater. **12**, 240 (2013).
[7] J. Sinha, M. Hayashi, A. J. Kellock, S. Fukami, M. Yamanouchi, H. Sato, S. Ikeda, S. Mitani, S.-h. Yang, S. S. P. Parkin, and H. Ohno, Enhanced interface perpendicular magnetic anisotropy in Ta|CoFeB|MgO using nitrogen doped Ta underlayers, Appl. Phys. Lett. **102**, 242405 (2013).
[8] S. Ikeda, K. Miura, H. Yamamoto, K. Mizunuma, H. D. Gan, M. Endo, S. Kanai, J. Hayakawa, F. Matsukura, and H. Ohno, A perpendicular-anisotropy CoFeB-MgO magnetic tunnel junction, Nat. Mater. **9**, 721 (2010).
[9] I. Mihai Miron, G. Gaudin, S. Auffret, B. Rodmacq, A. Schuhl, S. Pizzini, J. Vogel, and P. Gambardella, Current-driven spin torque induced by the Rashba effect in a ferromagnetic metal layer, Nat. Mater. **9**, 230 (2010).
[10] J. Torrejon, J. Kim, J. Sinha, S. Mitani, M. Hayashi, M. Yamanouchi, and H. Ohno, Interface control of the magnetic chirality in CoFeB/MgO heterostructures with heavy-metal underlayers, Nat. Commun. **5**, 4655 (2014).
[11] K. S. Ryu, L. Thomas, S. H. Yang, and S. Parkin, Chiral spin torque at magnetic domain walls, Nat. Nanotechnol. **8**, 527 (2013).
[12] S. Emori, U. Bauer, S. M. Ahn, E. Martinez, and G. S. D. Beach, Current-driven dynamics of chiral ferromagnetic domain walls, Nat. Mater. **12**, 611 (2013).
[13] G. Chen, T. Ma, A. T. N'Diaye, H. Kwon, C. Won, Y. Wu, and A. K. Schmid, Tailoring the chirality of magnetic domain walls by interface engineering, Nat. Commun. **4**, 2671 (2013).
[14] S. S. P. Parkin, M. Hayashi, and L. Thomas, Magnetic domain-wall racetrack memory, Science **320**, 190 (2008).
[15] M. Bode, M. Heide, K. von Bergmann, P. Ferriani, S. Heinze, G. Bihlmayer, A. Kubetzka, O. Pietzsch, S. Blugel, and R. Wiesendanger, Chiral magnetic order at surfaces driven by inversion asymmetry, Nature (London) **447**, 190 (2007).
[16] S. Heinze, K. von Bergmann, M. Menzel, J. Brede, A. Kubetzka, R. Wiesendanger, G. Bihlmayer, and S. Blugel, Spontaneous atomic-scale magnetic Skyrmion lattice in two dimensions, Nat. Phys. **7**, 713 (2011).
[17] N. Romming, C. Hanneken, M. Menzel, J. E. Bickel, B. Wolter, K. von Bergmann, A. Kubetzka, and R. Wiesendanger, Writing and deleting single magnetic Skyrmions, Science **341**, 636 (2013).
[18] H. Yang, A. Thiaville, S. Rohart, A. Fert, and M. Chshiev, Anatomy of Dzyaloshinskii-Moriya Interaction at Co/Pt Interfaces, Phys. Rev. Lett. **115**, 267210 (2015).
[19] X. Ma, G. Yu, X. Li, T. Wang, D. Wu, K. S. Olsson, Z. Chu, K. An, J. Q. Xiao, K. L. Wang, and X. Li, Interfacial control of Dzyaloshinskii-Moriya interaction in heavy

metal/ferromagnetic metal thin film heterostructures, Phys. Rev. B **94**, 180408 (2016).

[20] K. Zakeri, Y. Zhang, J. Prokop, T. H. Chuang, N. Sakr, W. X. Tang, and J. Kirschner, Asymmetric Spin-Wave Dispersion on Fe(110): Direct Evidence of the Dzyaloshinskii-Moriya Interaction, Phys. Rev. Lett. **104**, 137203 (2010).

[21] I. Gross, L. J. Martínez, J. P. Tetienne, T. Hingant, J. F. Roch, K. Garcia, R. Soucaille, J. P. Adam, J. V. Kim, S. Rohart, A. Thiaville, J. Torrejon, M. Hayashi, and V. Jacques, Direct measurement of interfacial Dzyaloshinskii-Moriya interaction in $X|$CoFeB$|$MgO heterostructures with a scanning NV magnetometer ($X =$ Ta, TaN and W), Phys. Rev. B **94**, 064413 (2016).

[22] V. E. Dmitrienko, E. N. Ovchinnikova, S. P. Collins, G. Nisbet, G. Beutier, Y. O. Kvashnin, V. V. Mazurenko, A. I. Lichtenstein, and M. I. Katsnelson, Measuring the Dzyaloshinskii-Moriya interaction in a weak ferromagnet, Nat. Phys. **10**, 202 (2014).

[23] S. Pizzini, J. Vogel, S. Rohart, L. D. Buda-Prejbeanu, E. Jué, O. Boulle, I. M. Miron, C. K. Safeer, S. Auffret, G. Gaudin, and A. Thiaville, Chirality-Induced Asymmetric Magnetic Nucleation in Pt/Co/AlO_x Ultrathin Microstructures, Phys. Rev. Lett. **113**, 047203 (2014).

[24] A. Thiaville, S. Rohart, É. Jué, V. Cros, and A. Fert, Dynamics of Dzyaloshinskii domain walls in ultrathin magnetic films, Europhys. Lett. **100**, 57002 (2012).

[25] M. Cubukcu, J. Sampaio, K. Bouzehouane, D. Apalkov, A. V. Khvalkovskiy, V. Cros, and N. Reyren, Dzyaloshinskii-Moriya anisotropy in nanomagnets with in-plane magnetization, Phys. Rev. B **93**, 020401 (2016).

[26] K. Di, V. L. Zhang, H. S. Lim, S. C. Ng, M. H. Kuok, J. Yu, J. Yoon, X. Qiu, and H. Yang, Direct Observation of the Dzyaloshinskii-Moriya Interaction in a Pt/Co/Ni Film, Phys. Rev. Lett. **114**, 047201 (2015).

[27] K. Di, V. L. Zhang, H. S. Lim, S. C. Ng, M. H. Kuok, X. Qiu, and H. Yang, Asymmetric spin-wave dispersion due to Dzyaloshinskii-Moriya interaction in an ultrathin Pt/CoFeB film, Appl. Phys. Lett. **106**, 052403 (2015).

[28] J. Cho, N.-H. Kim, S. Lee, J.-S. Kim, R. Lavrijsen, A. Solignac, Y. Yin, D.-S. Han, N. J. J. van Hoof, H. J. M. Swagten, B. Koopmans, and C.-Y. You, Thickness dependence of the interfacial Dzyaloshinskii-Moriya interaction in inversion symmetry broken systems, Nat. Commun. **6**, 7635 (2015).

[29] A. K. Chaurasiya, C. Banerjee, S. Pan, S. Sahoo, S. Choudhury, J. Sinha, and A. Barman, Direct observation of interfacial Dzyaloshinskii-Moriya interaction from asymmetric spin-wave propagation in W/CoFeB/SiO_2 heterostructures down to sub-nanometer CoFeB thickness, Sci. Rep. **6**, 32592 (2016).

[30] R. Soucaille, M. Belmeguenai, J. Torrejon, J. V. Kim, T. Devolder, Y. Roussigné, S. M. Chérif, A. A. Stashkevich, M. Hayashi, and J. P. Adam, Probing the Dzyaloshinskii-Moriya interaction in CoFeB ultrathin films using domain wall creep and Brillouin light spectroscopy, Phys. Rev. B **94**, 104431 (2016).

[31] G. Yu, L.-T. Chang, M. Akyol, P. Upadhyaya, C. He, X. Li, K. L. Wong, P. K. Amiri, and K. L. Wang, Current-driven perpendicular magnetization switching in Ta/CoFeB/[TaO_x or MgO/TaO_x] films with lateral structural asymmetry, Appl. Phys. Lett. **105**, 102411 (2014).

[32] G. Yu, P. Upadhyaya, K. L. Wong, W. Jiang, J. G. Alzate, J. Tang, P. K. Amiri, and K. L. Wang, Magnetization switching through spin-Hall-effect-induced chiral domain wall propagation, Phys. Rev. B **89**, 104421 (2014).

[33] S. Tacchi, R. E. Troncoso, M. Ahlberg, G. Gubbiotti, M. Madami, J. Ákerman, and P. Landeros, Interfacial Dzyaloshinskii-Moriya Interaction in Pt/CoFeB Films: Effect of the Heavy-Metal Thickness, Phys. Rev. Lett. **118**, 147201 (2017).

[34] D. Cortés-Ortuño and P. Landeros, Influence of the Dzyaloshinskii-Moriya interaction on the spin-wave spectra of thin films, J. Phys. Condens. Matter **25**, 156001 (2013).

[35] H. Yu, S. Zhu, X. Yang, X. Wang, H. Sun, and M. Huo, Synthesis of coral-like tantalum oxide films via anodization in mixed organic-inorganic electrolytes, PLoS One **8**, e66447 (2013).

[36] J. J. Colin, G. Abadias, A. Michel, and C. Jaouen, On the origin of the metastable β-Ta phase stabilization in tantalum sputtered thin films, Acta Mater. **126**, 481 (2017).

[37] R. Lo Conte, E. Martinez, A. Hrabec, A. Lamperti, T. Schulz, L. Nasi, L. Lazzarini, R. Mantovan, F. Maccherozzi, S. S. Dhesi, B. Ocker, C. H. Marrows, T. A. Moore, and M. Kläui, Role of B diffusion in the interfacial Dzyaloshinskii-Moriya interaction in Ta/$Co_{20}Fe_{60}B_{20}$/MgO nanowires, Phys. Rev. B **91**, 014433 (2015).

[38] J. Sinha, M. Gruber, M. Kodzuka, T. Ohkubo, S. Mitani, K. Hono, and M. Hayashi, Influence of boron diffusion on the perpendicular magnetic anisotropy in Ta$|$CoFeB$|$MgO ultrathin films, J. Appl. Phys. **117**, 043913 (2015).

[39] R. A. Khan, P. M. Shepley, A. Hrabec, A. W. J. Wells, B. Ocker, C. H. Marrows, and T. A. Moore, Effect of annealing on the interfacial Dzyaloshinskii-Moriya interaction in Ta/CoFeB/MgO trilayers, Appl. Phys. Lett. **109**, 132404 (2016).

[40] V. L. Zhang, K. Di, H. S. Lim, S. C. Ng, M. H. Kuok, J. Yu, J. Yoon, X. Qiu, and H. Yang, In-plane angular dependence of the spin-wave nonreciprocity of an ultrathin film with Dzyaloshinskii-Moriya interaction, Appl. Phys. Lett. **107**, 022402 (2015).